CSIRO PUBLISHING

Aust. J. Chem. **2013**, *66*, 370–380
http://dx.doi.org/10.1071/CH12421

Full Paper

Dithienylbenzothiadiazole-Based Donor-Acceptor Organic Semiconductors and Effect of End Capping Groups on Organic Field Effect Transistor Performance

Prashant Sonar,[A,D] *Samarendra P. Singh,*[A,C] *Ting Ting Lin,*[A] *and Ananth Dodabalapur*[A,B,D]

[A]Institute of Materials Research and Engineering, 3 Research Link Singapore 117602, Republic of Singapore.
[B]Permanent address: Microelectronics Research Center, The University of Texas at Austin, Austin, TX, 78758, USA.
[C]Current address: Shiv Nadar University, Greater Noida, 203207, India.
[D]Corresponding authors. Email: sonarp@imre.a-star.edu.sg; ananth.dodabalapur@engr.utexas.edu

Donor-Acceptor-Donor (D-A-D) based conjugated molecules 4,7-bis(5-(4-butoxyphenyl)thiophen-2-yl)benzo[*c*][1,2,5]thiadiazole (BOP-TBT) and 4,7-bis(5-(4-trifluoromethyl)phenyl)thiophen-2-yl)benzo[*c*][1,2,5]thiadiazole (TFP-TBT) using thiophene-benzothiadiazole-thiophene central core with trifluoromethyl phenyl and butoxyphenyl end capping groups were designed and synthesised via Suzuki coupling. Optical, electrochemical, thermal, and organic field effect transistor (OFET) device properties of BOP-TBT and TFP-TBT were investigated. Both small molecules possess two absorption bands. Optical band gaps were calculated from the absorption cut off to be in the range of 2.06–2.25 eV. Cyclic voltammetry indicated reversible oxidation and reduction processes and the highest occupied molecular orbital (HOMO) and the lowest unoccupied molecular orbital (LUMO) energy levels were calculated to be in the range of 5.15–5.40 eV and 3.25–3.62 eV, respectively. Upon testing both materials for OFET, trifluoromethylphenyl end capped material (TFP-TBT) shows n-channel behaviour whereas butoxyphenyl end capped material (BOP-TBT) shows p-channel behaviour. Density functional theory calculations correlated with shifting of HOMO-LUMO energy levels with respect to end capping groups. Vacuum processed OFET of these materials have shown highest hole carrier mobility of 0.02 cm^2/Vs and electron carrier mobility of 0.004 cm^2/Vs, respectively using Si/SiO_2 substrate. By keeping the central D-A-D segment and just by tuning end capping groups gives both p- and n-channel organic semiconductors which can be prepared in a single step using straightforward synthesis.

Manuscript received: 23 September 2012.
Manuscript accepted: 23 November 2012.
Published online: 9 January 2013.

Introduction

Organic field effect transistors (OFET) using small molecule organic semiconductors have received great attention due to their potential applications in low cost organic electronics.[1–4] OFET using organic semiconductors can potentially be utilised in applications such as drivers for large-area flexible displays or low end data storage smart cards. Organic materials possess the advantages of easy tuning of chemical structures, simpler processing and proven compatibility with plastic substrates. Additionally, their opto-electronic properties can be tuned easily by selecting appropriate conjugated building blocks in the backbone. Using such blocks, a library of both electron donor (hole transporting) and electron acceptor (electron transporting) materials with high thermal and chemical stability, facile processability, high charge carrier mobility, and controllable highest occupied molecular orbital (HOMO) and the lowest unoccupied molecular orbital (LUMO) energy levels can be prepared.[5–20] Among reported hole transporting and electron transporting materials, π-conjugated small molecules are an important category of organic semiconductors due to their well defined, monodisperse, discrete structure with synthetic reproducibility.[21–26] Small molecules are easier to purify and therefore result in less batch-to-batch variation. Small molecules have been studied extensively for OFET applications and among the most important materials classes are oligoacene and oligothiophene derivatives. Among all these materials, recently donor-acceptor-donor (D-A-D) based small molecules are becoming attractive candidates for OFET applications due to their strong intramolecular interactions.[27] Additionally, due to donor-acceptor charge transfer and low band gap, these

materials also have been used successfully as a donor component in organic photovoltaics (OPV).[28,29] The widely studied D-A-D based materials are mostly related with thiophene (D) and benzothiadiazole (A) building blocks due to their: (i) easy availability, (ii) possibility for structural modification, (iii) straightforward synthesis, and (iv) promising performance in organic electronic devices. The thiophene-benzothiadiazole conjugated system also has a benefit of forming self-assembled molecular assemblies in the solid state due to sulfur-nitrogen interactions.[27] Such intramolecular and intermolecular interactions through π-π stacking are expected to provide a good charge transportation pathway. Yamashita has reviewed several such classes of functional materials for p- and n-channel OFET applications.[27] Our group has also been working on D-A-D based materials over the past few years, trying to understand the structure-property relationship of these materials through fine tuning in the structural design and the effect on various optoelectronic properties (absorption, emission, energy level tuning, morphology, and charge transport behaviour).[30–32] These materials have been successfully used as active layers in OFET and organic photovoltaic devices. In this work, we report the design and synthesis of two D-A-D based materials 4,7-bis (5-(4-butoxyphenyl)thiophen-2-yl)benzo[*c*][1,2,5]thiadiazole (BOP-TBT) and 4,7-bis(5-(4-trifluoromethyl)phenyl)thiophen-2-yl)benzo[*c*][1,2,5]thiadiazole (TFP-TBT).[33,34] Although the synthesis of both compounds have been reported previously, there is no systematic comparison of both materials in terms of various properties (optical, electrochemical, thermal, and electrical) and their comparative performance in OFET. Both D-A-D materials have a similar conjugated backbone except for the difference in end capping groups. The rationale behind using alkoxy and trifluoromethyl substituted phenylene end capping groups for synthesising these D-A-D materials is to check the effect of electron donating and electron accepting end groups on the optical, electrochemical, and charge transport properties. These materials were characterised by various tools such as matrix-assisted laser desorption ionisation time-of-flight (MALDI-TOF), absorption and emission spectroscopy, cyclic voltammetry (CV), thermogravimetric analysis (TGA), differential scanning calorimetry (DSC), and by theoretical modelling. OFET made from BOP-TBT using vacuum deposition on octyltrichlorosilane (OTS) treated Si/SiO_2 substrate exhibited a hole mobility of 2×10^{-2} cm^2/Vs, whereas TFP-TBT deposited devices exhibited an electron mobility of 4×10^{-3} cm^2/Vs with gold source and drain electrodes. We demonstrated that by using different end capping groups with similar D-A-D core, we can create both p-channel and n-channel organic semiconductors with minimal synthetic effort. Due to high hole and electron mobility and low band gap, these materials are also potential candidates for bilayer OPV devices. The detailed synthesis, characterisation, and effect of end capping group on device performance are discussed below.

Experimental

Materials

All commercially available materials [(4-butoxyphenyl) boronic acid, 4-(trifluoromethyl)phenyl)boronic acid, tetrakis (triphenylphosphine)] were used as received unless otherwise noted. 4,7-Bis(5-bromothiophene-2-yl) benzothiadiazole was synthesised according to a published procedure.[35] All reactions were carried out using Schlenk techniques under an argon or nitrogen atmosphere in anhydrous solvents.

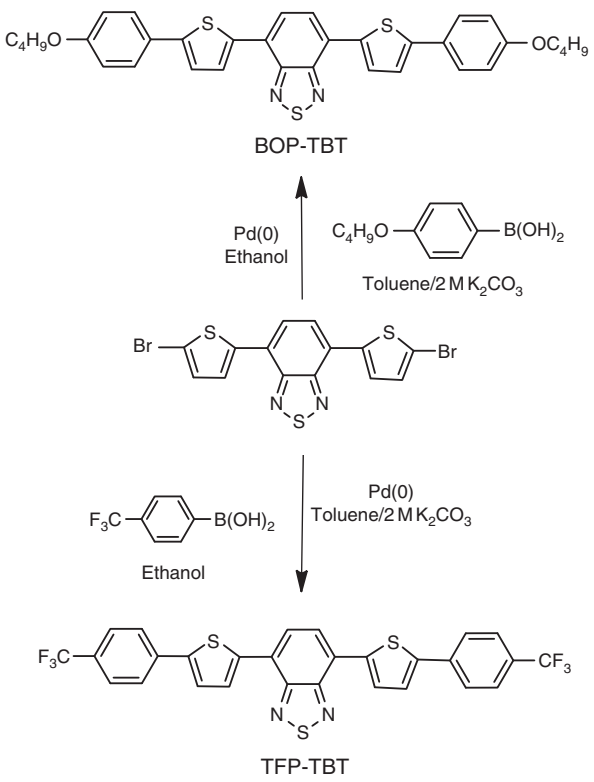

Scheme 1. Synthesis of D-A-D organic semiconductors BOP-TBT and TFP-TBT for organic field effect transistors.

Synthesis

4,7-Bis(5-(4-butoxyphenyl)thiophen-2-yl)benzo[c][1,2,5]thiadiazole (BOP-TBT)

To a Schlenk flask 4-(butoxyphenyl)boronic acid (0.425 g, 2.19 mmol) and 4, 7-bis(5-bromothiophene-2-yl) benzothiadiazole (0.400 g, 0.87 mmol), potassium carbonate (K_2CO_3) (2 M aqueous solution, 7 mL), and 3 mL of ethanol were dissolved in toluene (15 mL). The solution was purged with argon for 30 min, and then tetrakis(triphenylphosphine) palladium (20 mg, 0.017 mmol) was added instantly under argon flow. The reaction mixture was degassed by three freeze-pump thaw cycles and then stirred at 80°C for 48 h under argon. After completion of the reaction, toluene was removed and the product was precipitated in methanol; the resulting solid was filtered off and washed with copious amount of methanol. The crude product was purified using vacuum train sublimation at high temperature (250 to 300°C) yielding the pure product as dark red crystalline needles (77 % yield). Due to low solubility of the material we could not measure the NMR spectra. We confirmed the purity of the compound using elemental analysis and MALDI-TOF techniques.

Found: C 68.4, H 5.2, N 4.6, S 16.0. $C_{34}H_{32}N_2O_2S_3$ requires C 68.4, H 5.4, N 4.7, S 16.1 %. *m/z* (MALDI-TOF) 596.26; $[M]^+$ requires 596.16.

4,7-Bis(5-(4-trifluoromethyl)phenyl)thiophen-2-yl) benzo[c][1,2,5]thiadiazole (TFP-TBT)

4-(Trifluoromethyl)phenylboronic acid (0.500 g, 2.50 mmol), 4,7-bis(5-bromothiophene-2-yl)benzothiadiazole (0.500 g, 1.09 mmol), and sodium hydroxide (2 M aqueous solution, 5 mL) were added to a Schlenk flask and then dissolved in toluene (30 mL). The solution was purged with argon for 30 min,

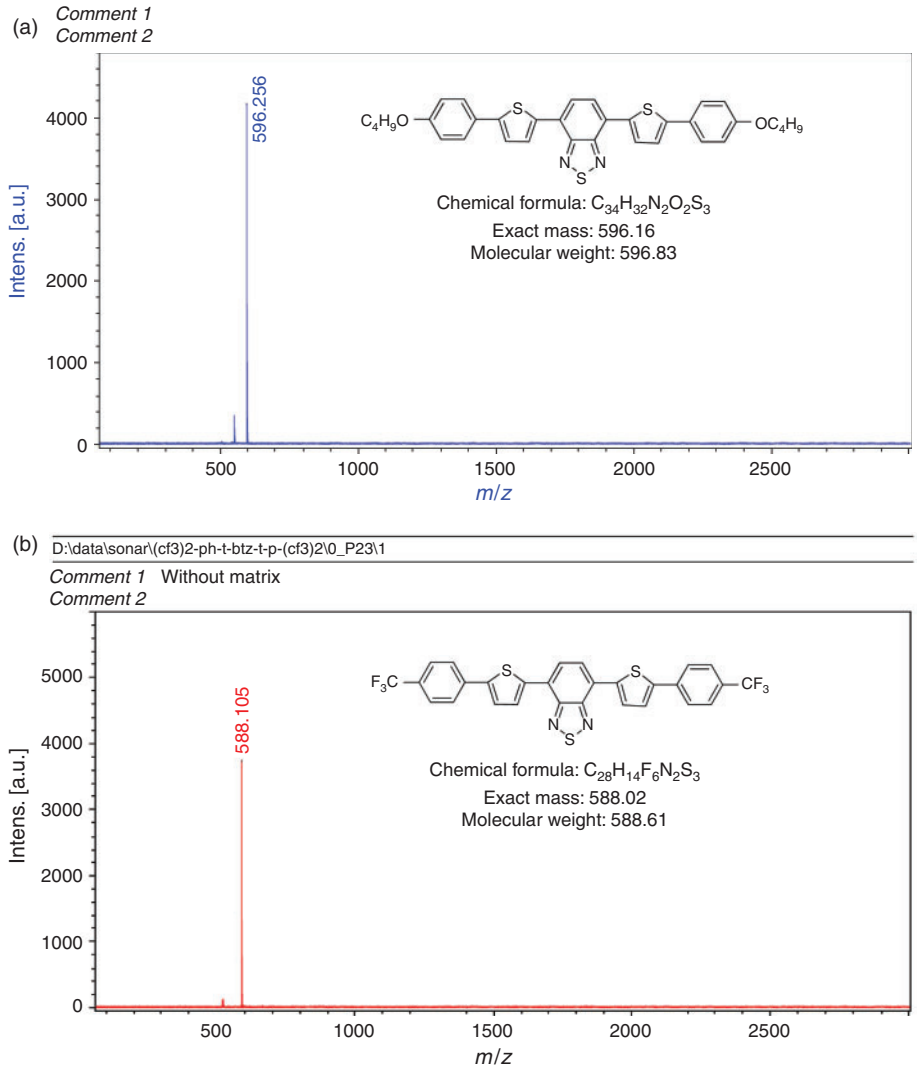

Fig. 1. Matrix assisted laser desorption/ionisation time-of-flight spectra of BOP-TBT and TFP-TBT organic semiconductors.

and then tetrakis(triphenylphosphine)palladium (150 mg, 0.12 mmol) was added quickly under argon flow. The reaction mixture was degassed by three freeze-pump thaw cycles and then stirred at 80°C for 48 h under argon. After completion of the reaction, toluene was removed and the product was precipitated in methanol; the resulting solid was filtered off and washed with copious amount of methanol. The crude product was purified using vacuum train sublimation at high temperature (250 to 300°C) yielding the pure product as a dark red crystalline solid (61 % yield). Again due to limited solubility of this material we could not perform NMR spectroscopy. Purity of the compound was confirmed by elemental analysis and MALDI-TOF techniques.

Found: C 57.0, H 2.2, N 4.6, S 15.7. $C_{28}H_{14}F_6N_2S_3$ requires C 57.1, H 2.4, N 4.8, S 16.3 %. *m/z* (MALDI-TOF) 588.10; $[M]^+$ requires 588.02.

Characterisation and Measurements

MALDI-TOF mass spectra were obtained on a Bruker Autoflex TOF/TOF instrument using dithranol as the matrix. Elemental analysis was conducted on a CHNSO Elemental Analyzer for quantitative measurements using FLASH EA-112 series by Thermo Electron Corporation. UV-Vis spectra were recorded on a Shimadzu model 2501-PC. DSC was carried out under nitrogen on a TA Instrument DSC Q100 with a scanning rate of 10°C min^{-1}. TGA was carried out using a TA Instrument TGA Q500 and a heating rate of 10°C min^{-1}. Cyclic voltammetry experiments were performed using an Autolab potentiostat (model PGSTAT30) by Echochimie. Measurements were recorded in dichloromethane solutions of BOP-TBT and TFP-TBT under argon at room temperature with a conventional three-electrode arrangement consisting of a platinum wire working electrode, a gold counter electrode, and an Ag/AgCl in 3 M KCl reference electrode, respectively. HOMO values were calculated from the corresponding oxidation onsets which were converted to saturated calomel electrode (SCE), based on an −4.4 eV SCE energy level relative to vacuum using ionisation potential, $IP = -(E_{ox\text{-}onset} + 4.4)$ eV. Likewise, LUMO levels were obtained from the reduction onsets via electron affinity, $EA = -(E_{red\text{-}onset} + 4.4)$ eV.

OFET Fabrication and Characterisation

Top contact/bottom gate OFET devices were fabricated using n^+-Si/SiO_2 substrates where n^+-Si and SiO_2 work as gate electrode and gate dielectric, respectively. Substrates were cleaned using ultrasonication in acetone, methanol, and

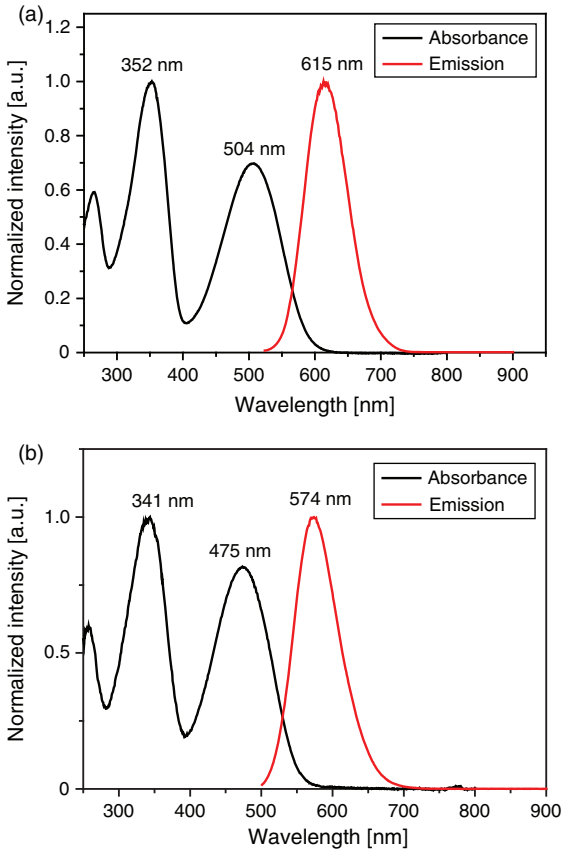

Fig. 2. Absorbance and emission spectrum of (a) BOP-TBT and (b) TFP-TBT D-A-D organic semiconductors.

de-ionized water consecutively. The cleaned substrates were dried under a nitrogen flow and heated at 100°C for 5 min. The substrates were then treated in UV-ozone for 20 min. The substrate was then kept in a desiccator with a few drops of OTS. The desiccator was evacuated for 3 min and placed in an oven at 110°C for 3 h. The substrate was removed from the desiccator, thoroughly rinsed with isopropanol, and dried under a nitrogen flow. For all sets of OFET, thin films of BOP-TBT and TFP-TBT were vacuum deposited on OTS treated Si/SiO_2 substrates. Patterned gold layers of thickness ~100 nm were deposited for use as source and drain electrodes through a shadow mask. For typical OFET devices reported here, the source-drain channel length and channel width were 100 µm and 1 mm, respectively. The device characteristics of the OFET were measured at room temperature under nitrogen with a Keithley 4200 parameter analyser.

Results and Discussion

Syntheses and Characterisation

The synthesis of dithienylbenzothiadiazole based D-A-D materials with different end capping groups is outlined in Scheme 1. First, dithienylbenzothiadiazole (93 % yield) was synthesised using commercially available 4,7-dibromobenzo[*c*][1,2,5]thiadiazole and 2-tributylstannylthiophene in dry *N*,*N*-dimethylformamide in presence of tetrakis(triphenyl phopshine) palladium catalyst at 80°C for 24 h by Stille coupling. Bromination of dithienylbenzothiadiazole was carried out using *N*-bromosuccinimide (NBS) in DMF at room temperature for 24 h producing 4,7-bis(5-bromothiophene-2-yl)benzothiadiazole (62 % yield). This dibromo derivative was used as a common block for synthesising the other two final compounds. Molecular

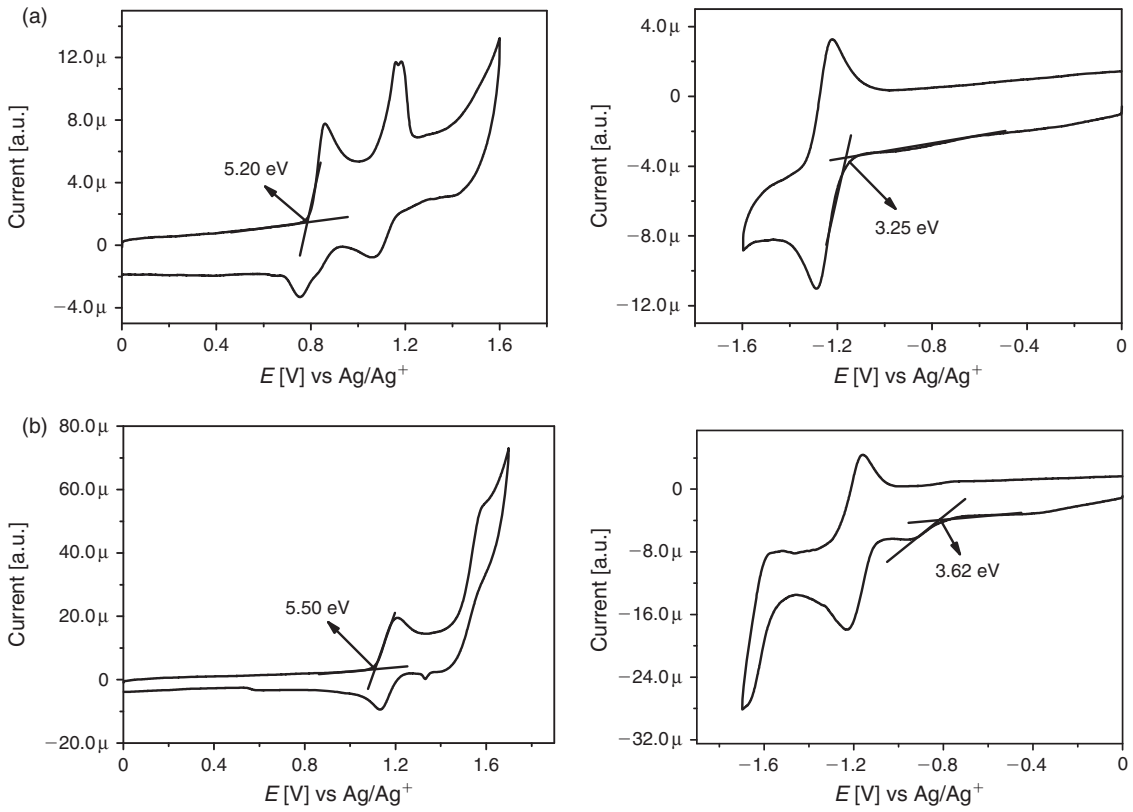

Fig. 3. Cyclic voltammogram analysis of (a) BOP-TBT and (b) TFP-TBT D-A-D organic semiconductors.

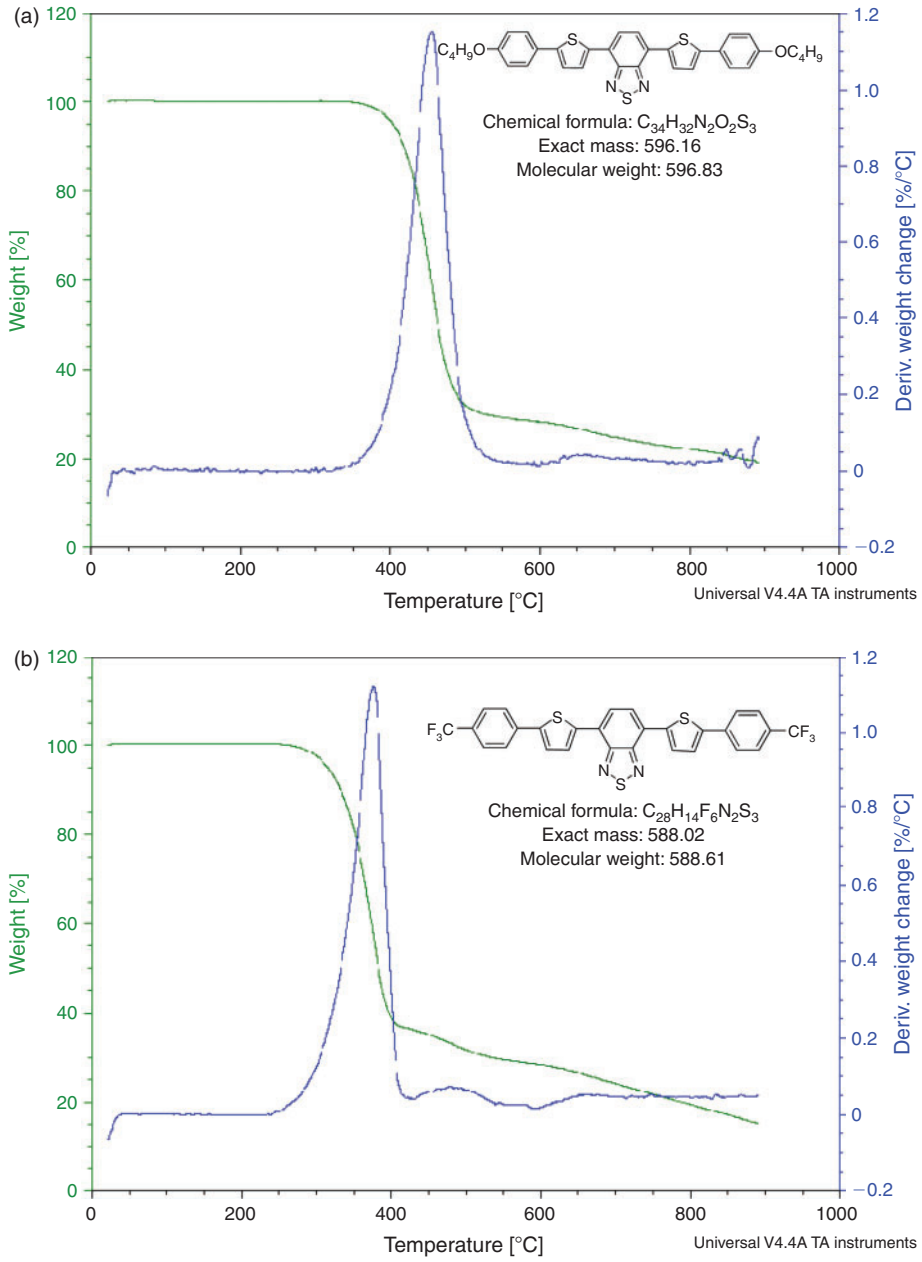

Fig. 4. Thermogravimetric analysis of (a) BOP-TBT and (b) TFP-TBT D-A-D organic semiconductors.

organic semiconductors 4,7-bis(5-(4-butoxyphenyl)thiophen-2-yl)benzo[*c*][1,2,5]thiadiazole (BOP-TBT) and 4,7-bis(5-(4-trifluoromethyl)phenyl)thiophen-2-yl)benzo[*c*][1,2,5]thiadiazole (TFP-TBT) were synthesised using 4-(butoxyphenyl)boronic acid and 4-(trifluoromethyl)phenyl)boronic acid with 4,7-bis(5-bromothiophene-2-yl)benzothiadiazole, as described in the Synthesis section, above. The respective MALDI-TOF of compounds BOP-TBT and TFP-TBT are shown in Fig. 1. Due to the low solubility of these organic semiconductors in organic solvents, we were unable to obtain ^{1}H or ^{13}C NMR spectra.

Optical Properties

The absorbance and photoluminescence spectra of BOP-TBT and TFP-TBT were measured in chloroform using 10^{-5} M solutions and are shown in Fig. 2a and 2b respectively. Both materials exhibit two absorption peaks, attributed to the thiophene constituent (lower wavelength region) and the charge transfer associated with thiophene-benzothiadiazole moieties (higher wavelength region) in the D-A-D backbone. In the lower wavelength region BOP-TBT and TFP-TBT exhibited absorption maxima at 352 and 341 nm respectively. In the longer wavelength region, BOP-TBT exhibits an absorption maximum at 504 nm whereas that for TFP-TBT is at 475 nm. Although the conjugated backbone of both materials have similar conjugated blocks, the 29 and 11 nm blue shift in longer and shorter wavelength region observed in TFP-TBT compared with BOP-TBT, respectively, is attributed to the stabilisation of the LUMO by the electron-withdrawing trifluoromethyl group. Similar observations have been reported recently for pyridine-benzothiadiazole based co-oligomers.[36] The optical band gaps calculated from the absorption cut off values are 2.06 and 2.25 eV for BOP-TBT and TFP-TBT respectively. The fluorescence spectra of BOP-TBT and TFP-TBT exhibit red photoluminescence maxima at 615 and 574 nm respectively.

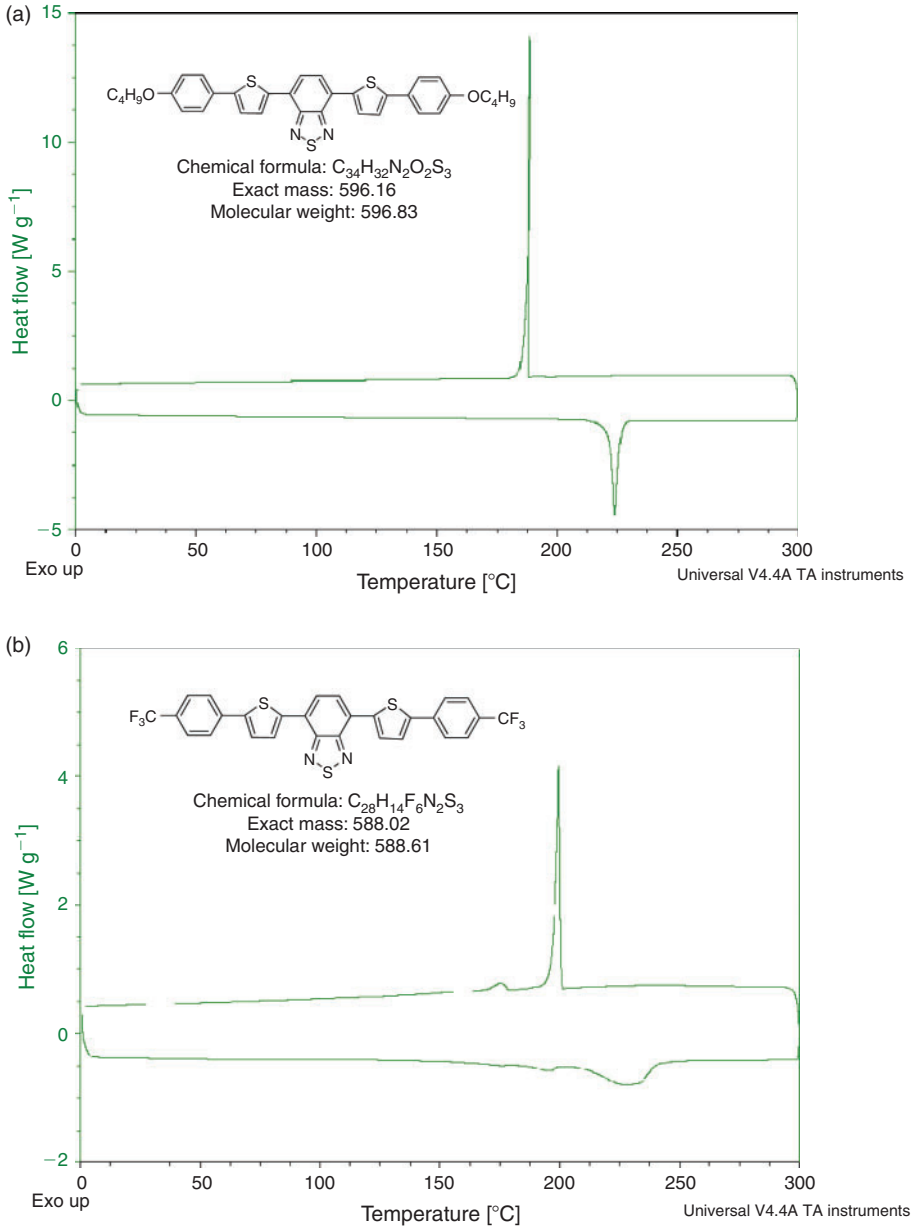

Fig. 5. Differential scanning calorimetry thermograms of (a) BOP-TBT and (b) TFP-TBT D-A-D organic semiconductors.

A blue shift of 41 nm is observed for TFP-TBT compared with BOP-TBT which is again related to stabilisation of the LUMO due to the electron withdrawing trifluoromethyl end capping group. Stokes shifts of 111 and 99 nm were observed for BOP-TBT and TFP-TBT respectively. This result clearly indicates that although possessing similar conjugated blocks in the backbone, the different alkyl end capping groups play a significant role in modulating photophysical properties.

Electrochemical Properties

The electrochemical properties of BOP-TBT and TFP-TBT were investigated by CV in order to estimate the electrochemical band gaps and HOMO/LUMO energy levels as a function of the end capping groups. All CV measurements were recorded at room temperature in dichloromethane (compounds were sparingly soluble indichloromethane) using a conventional three electrode configuration consisting of a platinum wire working electrode, a gold counter electrode, and an Ag/AgCl reference electrode under argon using tetrabutylammonium hexafluorophosphate as an electrolyte at a scan rate of $50\,\mathrm{mV\,s^{-1}}$. Both compounds exhibited reversible anodic and cathodic redox waves. HOMO-LUMO energy levels and the corresponding electrochemical band gaps of BOP-TBT and TFP-TBT were calculated from oxidation-reduction onset potentials. These onset potentials were converted to SCE and the corresponding IP and EA values were derived from the onset redox potentials, based on $-4.4\,\mathrm{eV}$ as the SCE energy level relative to vacuum ($\mathrm{EA} = E_{\text{red-onset}} + 4.4\,\mathrm{eV}$, $\mathrm{IP} = E_{\text{ox-onset}} + 4.4\,\mathrm{eV}$). The CV curves for BOP-TBT and TFP-TBT are shown in Fig. 3. BOP-TBT clearly exhibits two dominant oxidation peaks arising from two electron donating thiophene blocks whereas only one reduction peak is observed which is due to the single benzothiadiazole unit incorporated in the D-A-D backbone. TFP-TBT also shows one strong and one weak oxidation peak

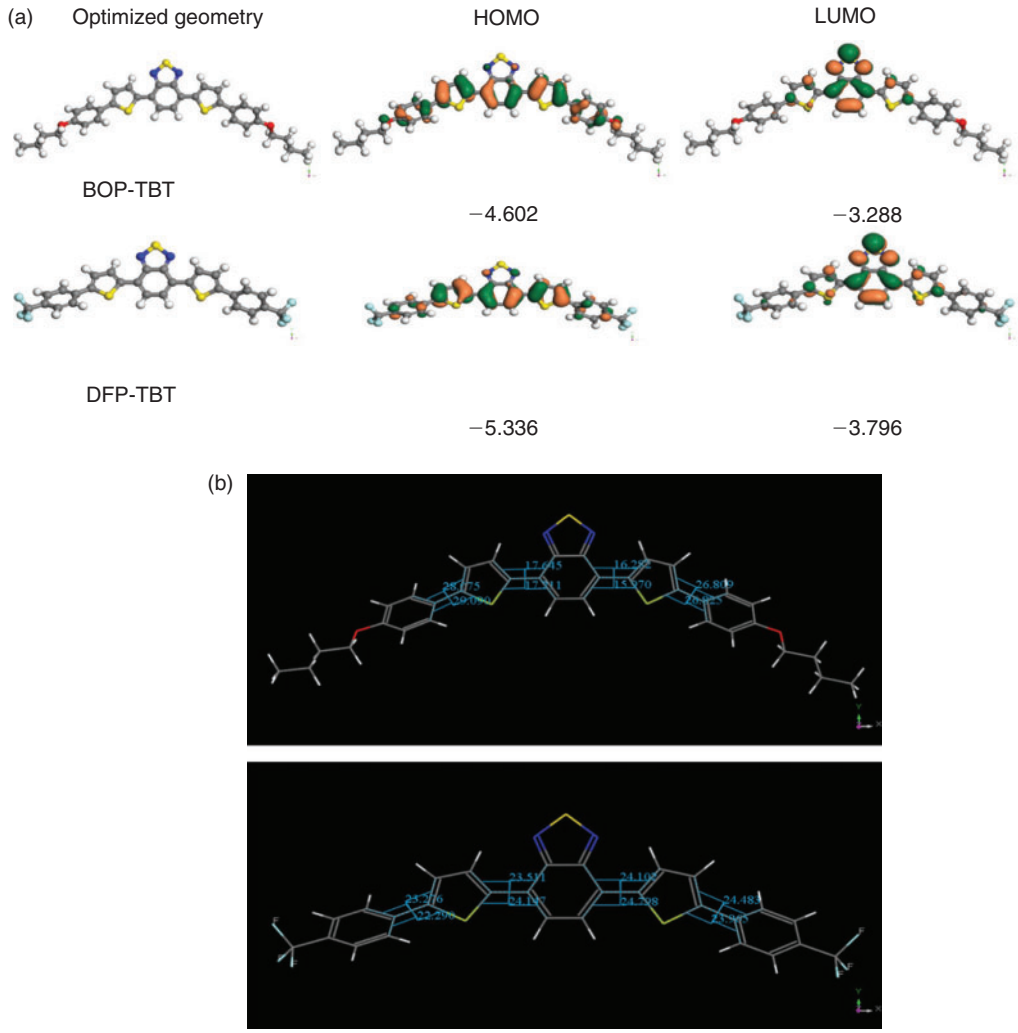

Fig. 6. The optimised geometries (a) and electron density isocontours of HOMO and LUMO of BOP-TBT and TFP-TBT and (b) the torsion angles between central D-A-D segment and alkyl substituted phenylene end capped group for the optimised structures obtained at GGA-PW91-dspp/dnp level and quality 'fine' using DMol^3 code.

whereas there are two reduction peaks due to benzothiadiazole (strong peak) and the trifluoromethyl group (weak peak). The oxidation onsets for BOP-TBT and TFP-TBT were observed at 0.8 and 1.10 V respectively. The HOMO values calculated for BOP-TBT and TFP-TBT are 5.20 and 5.50 eV while the LUMO values were determined to be 3.25 and 3.62 eV, respectively, calculated from the reduction onsets. The 0.30 and 0.37 eV lower values of HOMO and LUMO for TFP-TBT is due to the electron withdrawing effect of the trifluoromethyl group. From these values it can be clearly seen that HOMO-LUMO levels can be altered by using appropriate end capping groups, despite having the same conjugated backbone. Electrochemical band gaps calculated for BOP-TBT and TFP-TBT from the HOMO-LUMO differences are 1.95 and 1.88 eV respectively. These values are found to be in good agreement with the optical band gaps calculated from the UV-vis absorption onset.

Thermal Analysis

In order to determine the thermal stability and thermal transitions of these compounds, TGA and DSC were conducted under a nitrogen flow. TGA measures the amount and rate of change in the weight of a material as a function of temperature or time in a controlled atmosphere. Both BOP-TBT and TFP-TBT compounds show a 5 % weight loss (high decomposition temperature) at 400°C and 330°C, respectively, as shown in Fig. 4. This clearly indicates excellent thermal stability of the materials. Such a high stability is prerequisite for the purification of insoluble organic semiconductors using a vacuum sublimation method at high temperature. The high thermal stability of these compounds is due to the rigid backbone. Such thermally stable compounds allow fabrication of devices via vacuum sublimation without any decomposition. BOP-TBT shows better thermal stability than TFP-TBT due to the longer alkyl chain (butoxy) substituted on the phenyl ring compared to the shorter alkyl group (trifluoromethyl). This has also been confirmed by derivative weight loss curves for both compounds where the weight loss is most apparent. The DSC scans of BOP-TBT and TFP-TBT are depicted in Fig. 5 and this curve exhibits melting points at 222°C and 236°C respectively. BOP-TBT exhibits slightly lower melting temperature than TFP-TBT which is due to the longer alkyl chain (butoxy) substituted on the phenyl.

Density Functional Theory Electronic Structure Calculation

In order to study the planarity of the materials and the effects of end capping groups on electronic properties, density functional theory (DFT) calculations of their electronic state were

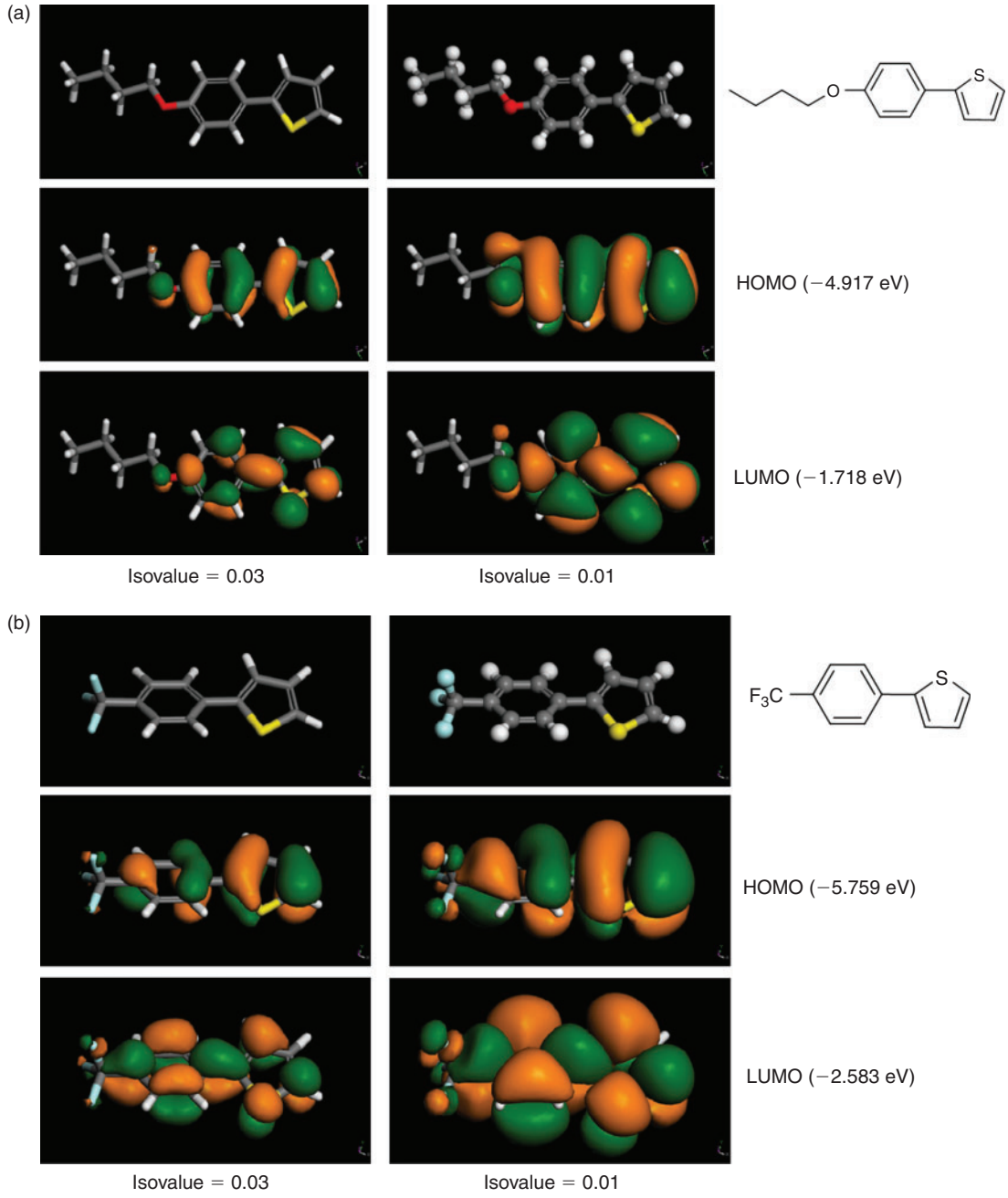

Fig. 7. The optimised geometries and electron density isocontours of HOMO and LUMO (measured at isovalue = 0.03 and 0.01) of end capping groups (a) butoxyphenyl and (b) trifluoromethylphenyl used for synthesising BOP-TBT and TFP-TBT respectively. These values are obtained at GGA-PW91-dspp/dnp level and quality 'fine' using DMol^3 code.

performed at the level of GGA-PW91-dspp/dnp using the DMol^3 module in the Materials Studio Modelling software package (Accelrys Inc.). The optimised geometries and electron density isocontours of HOMO and LUMO of BOP-TBT and TFP-TBT with their torsion angles (between central D-A-D segment and alkyl substituted phenylene end capped groups) are shown in Fig. 6. All the isocontour values are 0.02 atomic unit (a.u.). In all materials, the HOMO and LUMO are localised along the conjugated backbone. Localisation of the HOMO/LUMO orbital on such conjugated blocks has been commonly observed in previous theoretical studies.[31] The theoretical calculated HOMO-LUMO values and the band gaps of BOP-TBT and TFP-TBT are comparable with the experimental results and exhibit a similar trend (CV and optical data). The attachment of trifluoromethyl (an electron withdrawing group) to phenylene causes lowering of HOMO and LUMO levels of TFP-TBT compared with BOP-TBT in spite of having similar conjugated backbone. Such trends are expected due to higher electronegativity/electron affinity of the trifluoromethyl group compared with the butoxy group. The theoretically predicted HOMO and LUMO energy levels are ~0.51 to 0.73 eV higher than experimentally calculated values. The observed discrepancy of experimental and theoretical values are related with various effects such as effect of electrolyte, effect of solvent, and conformational order in the bulk state which is not taken into account in theoretical calculations. In order to confirm the effect

of end capping groups on HOMO-LUMO shifting of BOP-TBT and TFP-TBT, we also studied molecular modelling on individual trifluoromethylphenylene and butoxyphenylene end groups attached to thiophene. The optimised geometries and electron density isocontours at isovalue 0.01 and 0.03 of HOMO and LUMO of trifluoromethylphenylene and butoxyphenylene moieties attached to thiophene end groups are shown in Fig. 7. The HOMO and LUMO values for butoxyphenylene thiophene end group are calculated as −4.917 eV and −1.718 eV, whereas for trifluoromethylphenylene thiophene these values are −5.759 eV and −2.583 eV respectively. Just by changing the electron donating butoxy group with an electron withdrawing trifluoromethyl group, the LUMO value has been shifted by 0.87 eV. This theoretical data is significant to check the experimental results and we believe that theoretical modelling is a useful tool for designing and synthesising novel electron transporting organic semiconductors.

OFET Characteristics

The electrical properties of BOP-TBT and TFP-TBT were investigated by fabricating and characterising OFET devices using thin films of BOP-TBT and TFP-TBT. A bottom gate top-contact OFET device configuration was used to characterise the charge transport properties of BOP-TBT and TFP-TBT. The devices were fabricated on either p+-Si (or n+-Si) n^+-doped silicon wafers with a thermally grown silicon oxide layer (~200 nm) having a capacitance of ~17 nF cm^{-2}. The +-Si or n+-Si served as the gate electrode while the silicon oxide layer acted as the gate dielectric. The BOP-TBT and TFP-TBT were deposited on Si/SiO_2 substrate by vacuum deposition method. Gold was used as source and drain electrodes, and was thermally evaporated on top of the organic semiconductor thin film using a shadow mask. OFET devices have a channel length of 100 μm and a channel width of 1 mm. The evaluation of transistor performance was carried out in a glove box under nitrogen using a Keithley 4200 SCS semiconductor characterisation system. The output and transfer characteristics of OFET using BOP-TBT and TFP-TBT channel semiconductor are shown in Fig. 8 and Fig. 9 respectively. The carrier mobility in the saturated regime, μ_{sat}, is calculated according to Eqn (1):

$$I_{s.d.} = C_i\ \mu_{sat}\ (W/2L)(V_G - V_T)^2 \qquad (1)$$

where $I_{s.d.}$ is the drain current, W and L are, respectively, the semiconductor channel width and length, C_i is the capacitance per unit area of the gate dielectric, and V_G and V_T are, respectively, the gate voltage and threshold voltage. V_T of the device was determined from linear extrapolation of the linear fit of the $(I_{s.d.})^{1/2}$ versus V_G curve in the saturation regime at $I_D = 0$. The BOP-TBT based devices show p-channel performance with the best calculated hole mobility of 0.02 cm^2/Vs and threshold voltage of −33.0 Volts. The OFET devices fabricated on OTS treated Si/SiO_2 substrates have shown two orders of magnitude higher hole mobility as compared with the transistors fabricated on bare Si/SiO_2 substrates ($\mu_h = 6.2 \times 10^{-4}$ cm^2/Vs). Higher hole mobility exhibited in OFET devices fabricated on OTS treated substrates can be attributed to better packing of BOP-TBT thin films on self-assembled monolayer treated substrates. These mobility values are within the range of previously reported thiophene-benzothiadiazole based D-A-D small molecules.[27,30,31] The lower mobility of BOP-TBT compared with our earlier reported thiophene-benzothiadiazole based small molecules T4B1[30] might be due to the weak D-A interaction induced by the phenylene moiety (weak donor) than thiophene (strong donor). When the TFP-TBT molecule was used as a channel semiconductor in OFET devices, n-channel performance was observed with the best electron mobility 0.004 cm^2/Vs with threshold voltage 45.0 Volts calculated from the saturation regime. Both small molecules have similar conjugated backbone with the only difference being the alkyl group substituent. Due to the electron withdrawing trifluoromethyl group substitution on phenylene ring in TFP-TBT the LUMO is lowered resulting in n-channel performance, whereas BOP-TBT having butoxy group on phenylene shows p-channel performance. There are several reports of discrete p-channel and n-channel organic semiconductors but there are very few reports of making both p and n-channel organic semiconductors using a straightforward synthetic approach, using the same conjugated backbone, and just by tuning alkyl chain substitution. From these observations it is clear that different end capping group substitution is an effective synthetic method for the generation

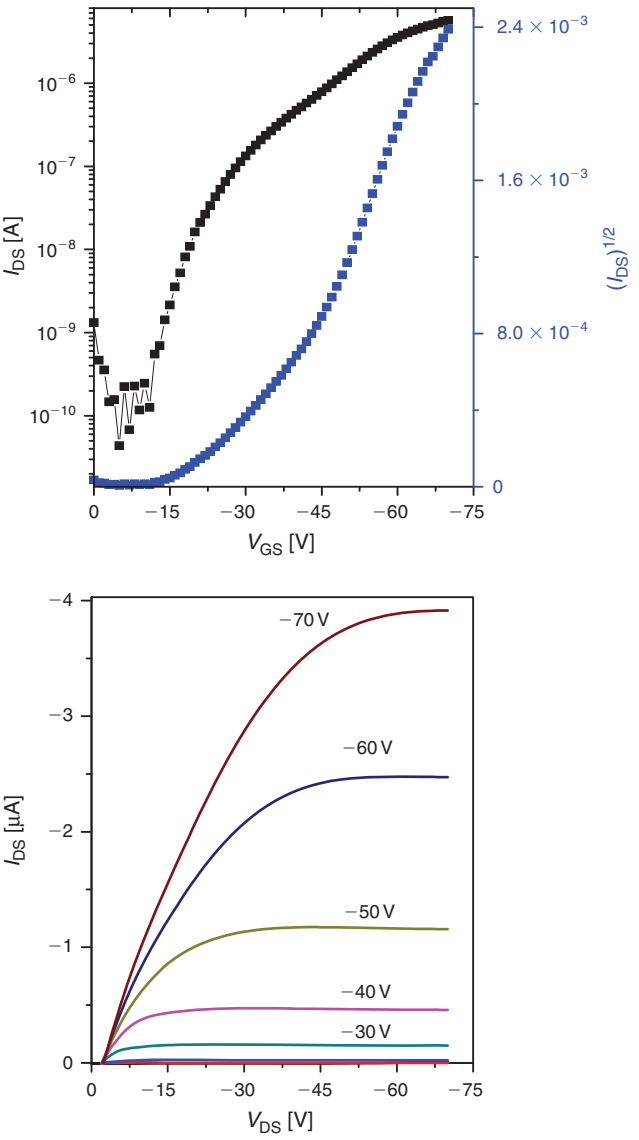

Fig. 8. Transfer (V_{GS} versus I_{DS}) and output (V_{DS} versus I_{DS}) characteristics of BOP-TBT based organic field effect transistors ($L = 100$ μm; $W = 1$ mm) on OTS treated p+-Si/SiO_2 substrate devices.

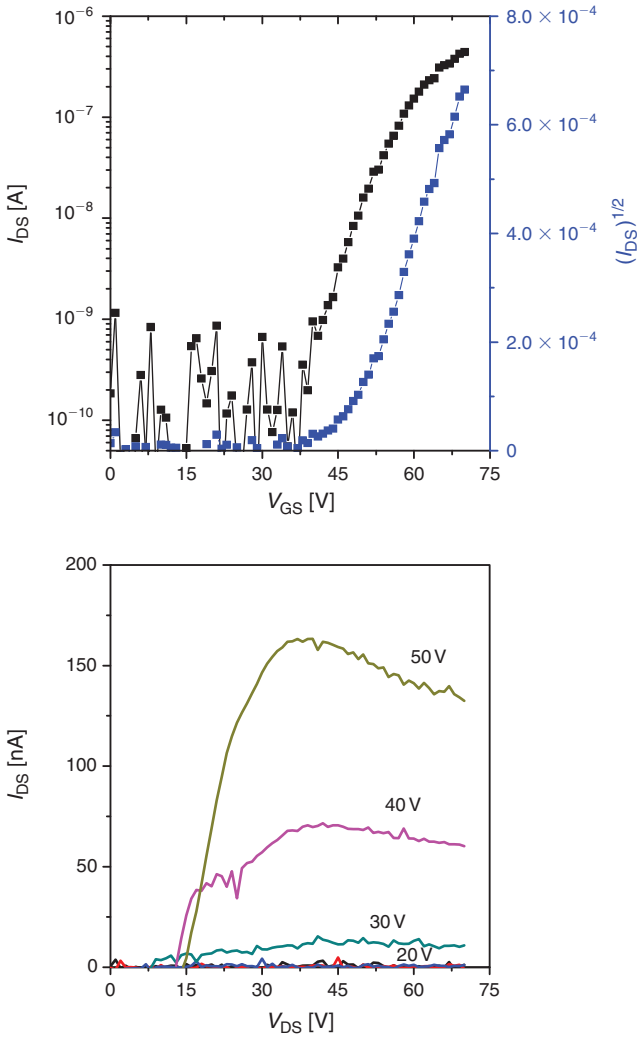

Fig. 9. Transfer (V_{GS} versus I_{DS}) and output (V_{DS} versus I_{DS}) characteristics of TFP-TBT based organic field effect transistors ($L = 100\,\mu m$; $W = 1$ mm) on OTS treated p+-Si/SiO_2 substrate devices.

of potential p- and n-channel semiconductors for high mobility OFET devices.

Conclusions

D-A-D based conjugated molecules BOP-TBT and TFP-TBT using a thiophene-benzothiadiazole-thiophene central core with butoxyphenyl and trifluoromethyl phenyl end capping groups have been designed, synthesised, and characterised. Both small molecules have shown optical band gaps ranging from 2.06 to 2.25 eV. HOMO and LUMO energy levels are calculated to be in the range of 5.15–5.4 eV to 3.25–3.62 eV from CV measurements. Upon testing both materials for OFET, triflormethylphenyl end capped material show n-channel behaviour, whereas the butoxyphenyl end capped material shows p-channel behaviour. Vacuum processed OFET of BOP-TBT and TFP-TBT have shown maximum hole mobility of 0.02 cm^2/Vs and electron mobility of 4×10^{-3} cm^2/Vs, respectively. Keeping the same central D-A-D conjugated segment and just tuning the end capping groups gives both p- and n-channel organic semiconductors in a single step using straightforward synthesis.

Acknowledgements

The authors acknowledge the Visiting Investigatorship Program (VIP) of the Agency for Science, Technology and Research (A*STAR), Republic of Singapore for financial support.

References

[1] Y. Shirota, H. Kageyama, *Chem. Rev.* **2007**, *107*, 953. doi:10.1021/CR050143+
[2] M. T. Lloyd, J. E. Anthony, G. G. Malliaras, *Mater. Today* **2007**, *10*, 34. doi:10.1016/S1369-7021(07)70277-8
[3] F. Garnier, *Acc. Chem. Res.* **1999**, *32*, 209. doi:10.1021/AR9800340
[4] M. Mas-Torrent, C. Rovira, *Chem. Soc. Rev.* **2008**, *37*, 827. doi:10.1039/B614393H
[5] S. Allard, M. Forster, B. Souharce, H. Thiem, U. Scherf, *Angew. Chem. Int. Ed.* **2008**, *47*, 4070. doi:10.1002/ANIE.200701920
[6] H. Klauk, *Organic Electronics: Materials, Manufacturing and Applications* **2006** (Wiley-VCH: Weinheim).
[7] K. Müllen, G. Wegner, *Electronic Materials: The Oligomer Approach* **1998** (Wiley-VCH: Weinheim).
[8] H. E. Katz, A. J. Lovinger, C. Klock, T. Siegrist, W. Li, Y. Y. Lin, A. Dodabalapur, *Nature* **2000**, *404*, 478. doi:10.1038/35006603
[9] B. Crone, A. Dodabalapur, Y. Y. Lin, R. W. Filas, A. LaDuca, R. Sarpeshkar, H. E. Katz, W. Li, *Nature* **2000**, *403*, 521. doi:10.1038/35000530
[10] B. Yoo, B. A. Jones, D. Basu, D. Fine, T. Jung, S. Mohapatra, A. Facchetti, K. Dimmler, M. R. Wasielewski, T. J. Marks, A. Dodabalapur, *Adv. Mater.* **2007**, *19*, 4028. doi:10.1002/ADMA.200700064
[11] M. H. Yoon, S. A. DiBenedetto, A. Facchetti, T. J. Marks, *J. Am. Chem. Soc.* **2005**, *127*, 1348. doi:10.1021/JA045124G
[12] A. Facchetti, Y. Deng, A. C. Wang, Y. Koide, H. Sirringhaus, T. J. Marks, R. H. Friend, *Angew. Chem. Int. Ed.* **2000**, *39*, 4547. doi:10.1002/1521-3773(20001215)39:24<4547::AID-ANIE4547>3.0.CO;2-J
[13] J. A. Letizia, A. Facchetti, C. L. Stern, M. A. Ratner, T. J. Marks, *J. Am. Chem. Soc.* **2005**, *127*, 13476. doi:10.1021/JA054276O
[14] S. Ando, R. Murakami, J. Nishida, H. Tada, Y. Inoue, S. Tokito, Y. Yamashita, *J. Am. Chem. Soc.* **2005**, *127*, 14996. doi:10.1021/JA055686F
[15] K. Ito, T. Suzuki, Y. Sakamoto, D. Kubota, Y. Inoue, F. Sato, S. Tokito, *Angew. Chem. Int. Ed.* **2003**, *42*, 10.
[16] C. D. Dimitrakopoulos, P. R. L. Malenfant, *Adv. Mater.* **2002**, *14*, 99. doi:10.1002/1521-4095(20020116)14:2<99::AID-ADMA99>3.0.CO;2-9
[17] D. J. Gundlach, Y.-Y. Lin, T. N. Jackson, S. F. Nelson, D. G. Schlom, *IEEE Electron Device Lett.* **1997**, *18*, 87. doi:10.1109/55.556089
[18] H. E. Katz, Z. Bao, S. L. Gilat, *Acc. Chem. Res.* **2001**, *34*, 359. doi:10.1021/AR990114J
[19] F. Garnier, A. Yassar, R. Hajlaoui, G. Horowitz, F. Deloffre, B. Servet, S. Ries, P. Alnot, *J. Am. Chem. Soc.* **1993**, *115*, 8716. doi:10.1021/JA00072A026
[20] D. J. Gundlach, Y.-Y. Lin, T. N. Jackson, D. G. Schlom, *Appl. Phys. Lett.* **1997**, *71*, 3853. doi:10.1063/1.120524
[21] Z. Bao, A. J. Lovinger, J. Brown, *J. Am. Chem. Soc.* **1998**, *120*, 207. doi:10.1021/JA9727629
[22] M. M. Shi, H. Z. Chen, J. Z. Sun, J. Ye, M. Wang, *Chem. Commun.* **2003**, *14*, 1710. doi:10.1039/B304141G
[23] Y. Sakamoto, T. Suzuki, M. Kobayashi, Y. Gao, Y. Fukai, Y. Inoue, F. Sato, S. Tokito, *J. Am. Chem. Soc.* **2004**, *126*, 8138. doi:10.1021/JA0476258
[24] C. Di, J. Li, G. Yu, Y. Xiao, Y. Guo, Y. Liu, X. Qian, D. Zhu, *Org. Lett.* **2008**, *10*, 3025. doi:10.1021/OL8008667
[25] M. Mas-Torrent, C. Rovira, *Chem. Soc. Rev.* **2008**, *37*, 827. doi:10.1039/B614393H
[26] C. R. Newman, C. D. Frisbie, D. A. da. S. Filho, J. L. Bredas, P. C. Ewbank, K. R. Mann, *Chem. Mater.* **2004**, *16*, 4436. doi:10.1021/CM049391X

[27] Y. Yamashita, *Sci. Technol. Adv. Mater.* **2009**, *10*, 024313. doi:10.1088/1468-6996/10/2/024313
[28] B. Walker, A. B. Tamayo, X.-D. Dang, P. Zalar, J. H. Seo, A. Garcia, M. Tantiwiwat, T.-Q. Nguyen, *Adv. Funct. Mater.* **2009**, *19*, 3063. doi:10.1002/ADFM.200900832
[29] J. A. Kong, E. Lim, K. K. Lee, S. Lee, S. H. Kim, *Sol. Energy Mater. Sol. Cells* **2010**, *94*, 2057. doi:10.1016/J.SOLMAT.2010.06.016
[30] P. Sonar, S. P. Singh, S. Sudhakar, A. Dodabalapur, A. Sellinger, *Chem. Mater.* **2008**, *20*, 3184. doi:10.1021/CM800139Q
[31] P. Sonar, S. P. Singh, P. Leclère, M. Surin, R. Lazzaroni, T. T. Lin, A. Dodabalapur, A. Sellinger, *J. Mater. Chem.* **2009**, *19*, 3228. doi:10.1039/B820528K
[32] P. Sonar, S. G. Santamaria, T. T. Lin, A. Sellinger, H. Bolink, *Aust. J. Chem.* **2012**, *65*, 1244. doi:10.1071/CH12171
[33] T. Kono, D. Kumaki, J. i. Nishida, T. Sakanoue, M. Kakita, H. Tada, S. Tokito, Y. Yamashita, *Chem. Mater.* **2007**, *19*, 1218. doi:10.1021/CM062889+
[34] G. Myhre, A. Sayyad, S. Mataka, S. Pau, *Appl. Phys. Lett.* **2011**, *99*, 091108. doi:10.1063/1.3631670
[35] J. Huang, Y. Xu, Q. Hou, W. Yang, M. Yuan, Y. Cao, *Macromol. Rapid Commun.* **2002**, *23*, 709. doi:10.1002/1521-3927(20020801)23:12<709::AID-MARC709>3.0.CO;2-E
[36] M. Akhtaruzzaman, M. Tomura, J. Nishida, Y. Yamashita, *J. Org. Chem.* **2004**, *69*, 2953. doi:10.1021/JO035800H